Carcinogenesis vol.25 no.8 pp.1–11, 2004
DOI: 10.1093/carcin/bgh173

Oligonucleotide microarray analysis of gene expression in neuroblastoma displaying loss of chromosome 11q

L.McArdle[1,2], M.McDermott[3], R.Purcell[3], D.Grehan[3], A.O'Meara[4], F.Breatnach[4], D.Catchpoole[5], A.C.Culhane[2], I.Jeffery[2], W.M.Gallagher[2] and R.L.Stallings[1,2,6]

[1]National Centre for Medical Genetics, Our Lady's Hospital for Sick Children, Crumlin, Dublin 12, Ireland, [2]Conway Institute of Biomolecular and Biomedical Research, University College Dublin, Dublin, Ireland, [3]Department of Histopathology, Our Lady's Hospital for Sick Children, Crumlin, Dublin 12, Ireland, [4]Department of Oncology, Our Lady's Hospital for Sick Children, Crumlin, Dublin 12, Ireland and [5]Tumor Bank, The Children's Hospital at Westmead, Sydney, Australia

[6]To whom correspondence should be addressed
Email: ray.stallings@olhsc.ie

A number of distinct subtypes of neuroblastoma exist with different genetic abnormalities that are predicative of outcome. Whole chromosome gains are usually associated with low stage disease and favourable outcome, whereas loss of 1p, 3p and 11q, unbalanced gain of 17q and *MYCN* amplification (MNA) are indicative of high stage disease and unfavourable prognosis. Although MNA and loss of 11q appear to represent two distinct genetic subtypes of advanced stage neuroblastoma, a detailed understanding of how these subtypes differ in terms of global gene expression is still lacking. We have used metaphase comparative genomic hybridization (CGH) analysis in combination with oligonucleotide technology to identify patterns of gene expression that correlate with specific genomic imbalances found in primary neuroblastic tumours and cell lines. The tumours analysed in this manner included a ganglioneuroma, along with various ganglioneuroblastoma and neuroblastoma of different stages and histopathological classifications. Oligonucleotide microarray-based gene expression profile analysis was performed with Affymetrix HU133A arrays representing ~14 500 unique genes. The oligonucleotide microarray results were subsequently validated by quantitative real-time PCR, immunohistochemical staining, and by comparison of specific gene expression patterns with published results. Hierarchical clustering of gene expression data distinguished tumours on the basis of stage, differentiation and genetic abnormalities. A number of genes were identified whose patterns of expression were highly correlated with 11q loss; supporting the concept that loss of 11q represents a distinct genetic subtype of neuroblastoma. The implications of these results in the process of neuroblastoma development and progression are discussed.

Abbreviations: CGH, comparative genomic hybridization; COA, correspondence analysis; MNA, *MYCN* amplification; RMA, Robust Multi-Chip Average; TMA, tissue microarray.

Introduction

Neuroblastoma is characterized by diverse clinical behaviours ranging from complete regression of the disease to rapid tumour progression and death (see ref. 1 for review). Patient age and stage of disease are important factors in determining outcome. Infants often experience complete regression of their disease while the majority of children over 1.5 years of age have metastatic disease at diagnosis and a poor prognosis despite intensive therapy. Identification of recurrent genomic abnormalities has allowed classification of neuroblastic tumours into distinct genetic subtypes that are predictive of clinical behaviour. Tumours that have a high propensity for spontaneous regression usually exhibit only whole chromosome gains and losses, whereas metastatic neuroblastoma is characterized by numerous recurrent structural chromosome abnormalities.

The most common structural chromosome abnormalities are associated with aggressive clinical behaviour and include loss of chromosome 1p and 11q, *MYCN* amplification (MNA) and unbalanced gain of the long arm of chromosome 17 (2–6). An inverse relationship exists between MNA and 11q loss, indicating that these abnormalities represent distinct genetic subtypes of advanced stage neuroblastoma (5,7,8). These two major genetic subtypes are further defined by loss of 1p in the MNA subtype and loss of 3p in 11q- tumours (4,6,8). Unbalanced gain of 17q material is the most common abnormality detected in advanced stage disease, occurring in 80–90% of advanced stage tumours irrespective of MNA or 11q loss status (2,3,5).

The numerous genes and genetic pathways affected by amplification of the *MYCN* transcription factor are only just beginning to be identified (9); moreover, the genes targeted by the many other recurrent chromosomal imbalances, such as loss of 11q, are unknown. Global analysis of gene expression patterns using contemporary technologies holds great promise for identifying the molecular determinants of neuroblastoma pathogenesis. Indeed, serial analysis of gene expression (SAGE) studies of MNA neuroblastoma have revealed that *MYCN* enhances the expression of a number of genes involved with protein synthesis (10), while other SAGE studies have revealed that the *MEIS1* oncogene is over-expressed in 25% of neuroblastoma (11). Detailed SAGE studies for the purpose of classifying neuroblastoma or for relating specific chromosomal imbalances in these tumour types to patterns of gene expression have not been carried out.

The first microarray-based gene expression profiling study of neuroblastoma was published by Khan *et al*. (12), who demonstrated that different small round blue cell tumours, including neuroblastoma, rhabdomyosarcoma, non-Hodgkin lymphoma and Ewing tumours, could be distinguished on the basis of their patterns of gene expression. Subsequent microarray studies have facilitated class separation of differentiating neuroblastoma tumours from poorly differentiated tumours

(13), as well as high-risk tumours from low-risk tumours (14,15).

Recent expression microarray studies of breast cancer cells indicate that chromosomal imbalances have a significant impact on global gene expression patterns (16,17) and support the view that aneuploidy plays a major role in carcinogenesis (18). We have used high-density oligonucleotide array-based gene expression profiling to identify transcripts that are differentially expressed in the 11q-, MNA and hyperdiploid subtypes of neuroblastoma. In addition, the expression patterns of genes associated with benign neuroblastic tumours (ganglioneuroma) was compared with patterns from neuroblastoma. Our study represents the first oligonucleotide microarray-based gene expression profiling study of primary neuroblastic tumours and cell lines, which have also been characterized by metaphase comparative genomic hybridization (CGH) analysis. We report that the major genetic subtypes of advanced stage tumours can be differentiated on the basis of gene expression profiles and that distinct patterns of gene expression can be correlated with specific genomic alterations. A number of genes were identified which probably exhibit tumour stage-specific expression profiles. Finally, the implications of our studies with respect to understanding the molecular basis of neuroblastoma progression are discussed.

Materials and methods

Neuroblastoma tissue and cell lines

CGH analysis was performed on all primary tumours, with 20 patients presenting to the Oncology Department of Our Lady's Hospital for Sick Children, Dublin and two cases (86 and 67) from The Children's Hospital at Westmead, Sydney. Neuroblastoma tissue was snap frozen in liquid nitrogen immediately after surgery and stored at −80°C until analysis. The tumours included one ganglioneuroma, four ganglioneuroblastoma ($n = 2$ stage 2 and $n = 2$ stage 4) and 17 neuroblastomas at stage 1 ($n = 1$), stage 2 ($n = 6$), stage 3 ($n = 1$), stage 4 ($n = 8$) and stage 4s ($n = 1$). The SK-N-AS and Kelly (N206) cell lines were obtained from the European Collection of Cell Cultures (http://www.ecacc.org.uk/).

Histology from each specimen was reviewed and tumours graded according to the International Neuroblastoma Pathology Classification (INPC) system (Table I) (19,20). All tumours were obtained at diagnosis prior to chemotherapy. We were able to provide pathologic assessment of some of the ganglioneuroblastoma material by the use of tissue blocks mirroring the material used for RNA extraction in two of the ganglioneuroblastoma cases (nos 56 and 59). Examination of these tissue sections showed that the sampled material in case 56 was devoid of Schwann cells, being composed of 100% neuroblastic tissue, while the sample from case 59 was composed of 80% neuroblastic tissue and 20% Schwann cells. Case 27 exhibited an almost completely uniform histological appearance, with the vast bulk of the tumour devoid of Schwann cells and composed of 100% neuroblastic tissue. It's designation as a ganglioneuroblastoma was based on the presence of a thin peripheral of ganglioneuromatous tissue not sampled in the material submitted for cytogenetics. Case 57 also exhibited a uniform histological picture, being composed of 90% Schwann cells and 10% neuroblastic cells.

CGH analysis

Comparative genomic hybridization experiments were carried out as described previously (22). CGH data on some cases has been published previously (6,21).

Oligonucleotide microarray analysis

Affymetrix HU133A GeneChips (Santa Clara, CA) were used for all experiments. Following tissue homogenization, total RNA was isolated via a Trizol-based extraction method (Life Technologies). The targets for Affymetrix microarray analysis were prepared as described by the manufacturer. Approximately 7.5 μg total RNA was used as starting material for the cDNA preparation. Single- and double-stranded cDNA synthesis was performed using the Superscript Choice System (Life Technologies) and an oligo-dT primer containing a T7 RNA polymerase promoter site (Genset). Biotin-labelled cRNA was prepared using the BioArray High Yield RNA Transcript labelling kit (Enzo). Approximately 15 μg cRNA was fragmented at 94°C for 35 min prior to hybridization. The quality of labelled target was initially assessed using Genechip Test3 arrays. Hybridization on the expression arrays was for 16 h at 45°C. Following hybridization, standard washing and staining procedures were carried out on an Affymetrix Fluidics Station 640. Processed arrays were examined using a GeneChip Scanner 2500 and resultant image data managed via Affymetrix Microarray Suite software version 5.0 (MAS5.0). All of the raw data for each tumour is available at http://www.ebi.ac.uk/arrayexpress/ (accession number E-MEXP-83).

Statistical analysis methods

The overall data from all array experiments was scaled to a global intensity of 100 using MAS5.0 in order to control for within-array variation in intensity. The scaled data was then imported into GeneSpring software version 6 (Silicon Genetics, Redwood City, CA). Before applying clustering analysis, transcripts were normalized using GeneSpring by dividing the value for each transcript by the median of its measurements in all samples in order to account for the difference in detection efficiency between spots. A number of different filtering criteria were applied to the expression data to exclude transcripts that were not well measured. For this purpose, those probe sets that displayed an absent call in all 24 samples (22 tumours and two cell lines) were removed, resulting in a 16 654 transcript list. The next filtering steps involved selecting transcripts, which had a raw value of 100 in at least three samples, exhibited a 'Present' call in at least three samples, and whose corresponding transcripts varied in abundance by at least 3-fold from their median abundance in at least two samples. This combined filtering process yielded a more refined list of 2660 differentially expressed transcripts. Both the 16 654 and 2660 transcript lists were subjected to unsupervised two-way hierarchical cluster analysis, using the Pearson correlation as a similarity metric.

All subsequent analysis was performed using the Bioconductor and ADE4 packages of the open source statistical analysis software R. Recent spike-in and dilution studies have shown that the default expression measure provided by Affymetrix Microarray Suite software can be significantly improved using statistical models such as the Robust Multi-Chip Average (RMA) method (23). Thus, raw Affymetrix intensity measurements of all probe sets were converted into expression measurements using the RMA module. The C implementation of RMA in the Bioconductor package, Affy, was used, which normalizes the corrected perfect match probes using quantile normalization and calculates expression measures using median polish. These RMA expression measurements were also compared with MAS5.0 (Affymetrix, 2001) and Li and Wong DChip expression measurements (24) (data not shown). Average linkage hierarchical cluster analysis, using the Pearson correlation as a measure of similarity, of each of these datasets produced clusters of MNA and 11q- tumours, similar to that described in Figure 1 when the 16 654 gene subset was examined (data not shown).

Hierarchical cluster analysis partitions data into discrete hierarchical groups based on the trends within the data, but has the disadvantage that it sometimes forces arbitrary divisions of a dataset even when presented with continuous variation. Therefore, in addition to hierarchical cluster analysis, the data were analysed using correspondence analysis (COA) (25). COA is an ordination technique that identifies the major trends in the data and distributes samples/genes along continuous axes in accordance with these trends. Since COA does not assume that the data falls into discrete clusters, clusters with continuous variation (gradients) can be distinguished from discrete groupings in the data. COA was performed using the ade4 package in R (27), and similar patterns in the data were observed when results were compared with those obtained from hierarchical clustering analysis. In COA, the GN/GNB (ganglioblastoma/ganglioneuroblastoma), MNA and 11q- tumours were observed on the first, second and third axes, respectively, and thus represented the most significant features in the data (data not shown).

A number of methods were used to identify the genes that were most strongly associated with these groupings (GN/GNB, MNA and 11q- tumours). We used the supervised analysis method, between group analysis (BGA) (26), to rank the genes most associated with each of these clusters. BGA was performed using the ade4 module in R (27) and provided lists of genes most associated with each cluster. We used permutation-based modified *t*-tests to provide further confidence in these results. Differential gene expression was analysed using a two-sample Welch *t*-statistic (unequal variances) with the step down re-sampling procedure, MaxT (28), which provided permutation adjusted *P*-values that control for increased type I (false positive) error associated with multiple testing of large numbers of variables. These adjusted *P*-values were computed from 10 000 permutations using the multtest package in Bioconductor. However, MaxT permutation adjusted *P*-values required lots of permutations, and we were limited by the subgroups size in the data. Thus, differential gene expression associated with each group was tested using Significance Analysis of Microarrays (SAM) (29,30). SAM assigns a score to each gene based on the change in gene

Table I. CGH analysis of neuroblastoma pre-treatment tumours

Case	INSS	INPC	Primary site	INPC prognostic category	CGH result	FR[a] 2p24	Age[b]
26	1	NB poorly differentiated	Abdominal	Unfavourable	**enh** 6q15-q23, 17q21qter; **dim** 3p21pter, 4p14pter, 11q14qter		10 m
18	2	NB poorly differentiated	Cervicothoracic	Favourable	**enh** 5, 6, 12, 17 and 18		1w
27	2a	GNB atypical, nodular	Abdominal	Unfavourable	**enh** 11p11-p14, 13q, 17q21qter, 18; **dim** 1p32pter, 9q32qter, 11q21qter, 12q23qter		36 m
36	2a	NB poorly differentiated	Thoracic	Unfavourable	**enh** 1,2,6,7,9,12		1 m
30	2	NB differentiating	Abdominal	Favourable	**enh** 7		10 m
52	2	NB poorly differentiated	Thoracic	Unfavourable	**enh** 6pter-q22; 17q12qter; **dim** 11q14qter		16 m
54	2	NB poorly differentiated	Thoracic	Unfavourable	**enh 13**, **17**,		9 m
53	2	NB undifferentiated (pleomorphic subtype)	Abdominal	Unfavourable	**enh** 2pter-q33, 7q21qter, 17q12qter; **amp** 2p23-p24; **dim** 1p32pter, 10q21qter, 16q22qter	1.5	37 m
59	2	GNB, intermixed	pelvic	Favourable	Normal profile; hyperdiploidy by FISH		37 m
25	3	NB poorly differentiated	Abdominal	Unfavourable	**enh** 7, 8, 17, 18		73 m
42	4s	NB poorly differentiated	Abdominal	Unfavourable	**enh** 2p21pter, 3q26.1qter, 17q22qter; **amp 2p23p24**; **dim** 1p33pter	1.5	5 m
31	4	NB poorly differentiated	Abdominal	Unfavourable	**enh** 7q, 13q14-q22, 17q21qter; **dim** 3p21pter, 11q14qter		23 m
35	4	NB poorly differentiated	Cervico thoracic	Unfavourable	**enh** 7q22qter, 11pter-q13, 17q11.2qter; **dim** 5p13pter, 11q14qter		29 m
37	4	NB poorlydifferentiated	Thoracoabdominal	Unfavourable	**enh** 5q23qter, 7, 11pter-q13, 12, 17q10qter,18; **dim** 3p21pter, 11q22qter		22 m
45	4	NB poorlydifferentiated	Abdominal	Unfavourable	**enh** 2p21pter, 7q21qter, 8q22qter, 11q13-pter, 12q22qter, 13q32qter, 14, 17q21qter; **dim** 5p13pter, 11q14qer		35 m
47	4	NB poorly differentiated	Abdominal	Unfavourable	**enh** 17q21qter; **dim** 11q14qter, Xp		10 m
48	4	NB poorly differentiated	Abdominal	Unfavourable	**enh** 11p, 17q21qter; **dim** 3p21pter, 11q14qter		11 m
55	4	NB poorly differentiated	Abdominal	Unfavourable	**enh** 1q, 2, 6, 7, 12, 17, 18; **amp** 2p23p24, 6q26q21, **dim** 1p10pter, 13, 14, 15	2.0	77 m
56	4	GNB, atypical nodular	Abdominal	Unfavourable	Normal Profile; Hyperdiploidy by FISH		36 m
57		Ganglioneuroma	Abdominal	Benign	Normal profile		14y2 m
67	4	Ganglioneuroblastoma	Abdominal	Unfavourable	**enh** 5q23qter, 7q22qter, 17q21qter, 18, **dim** 6q22qter, 11q14qter		43 m
86	4	NB differentiating	Abdominal	Unfavourable	**enh** 2p13pter; **amp** 2p23p24, 11q13qter **dim** 1p32pter; 11q14qter	1.3	8 m

INPC = International Neuroblastoma Pathology Classification; INSS = International Neuroblastoma Staging System; NB = neuroblastoma; GNB = ganglioneuroblastoma. **enh** = enhanced green to red fluorescent ratio of chromosomal region (gain); **dim** = diminished green to red fluorescent ratio of chromosomal region (loss).
[a]Age at diagnosis; y = years; m = months; w = weeks.

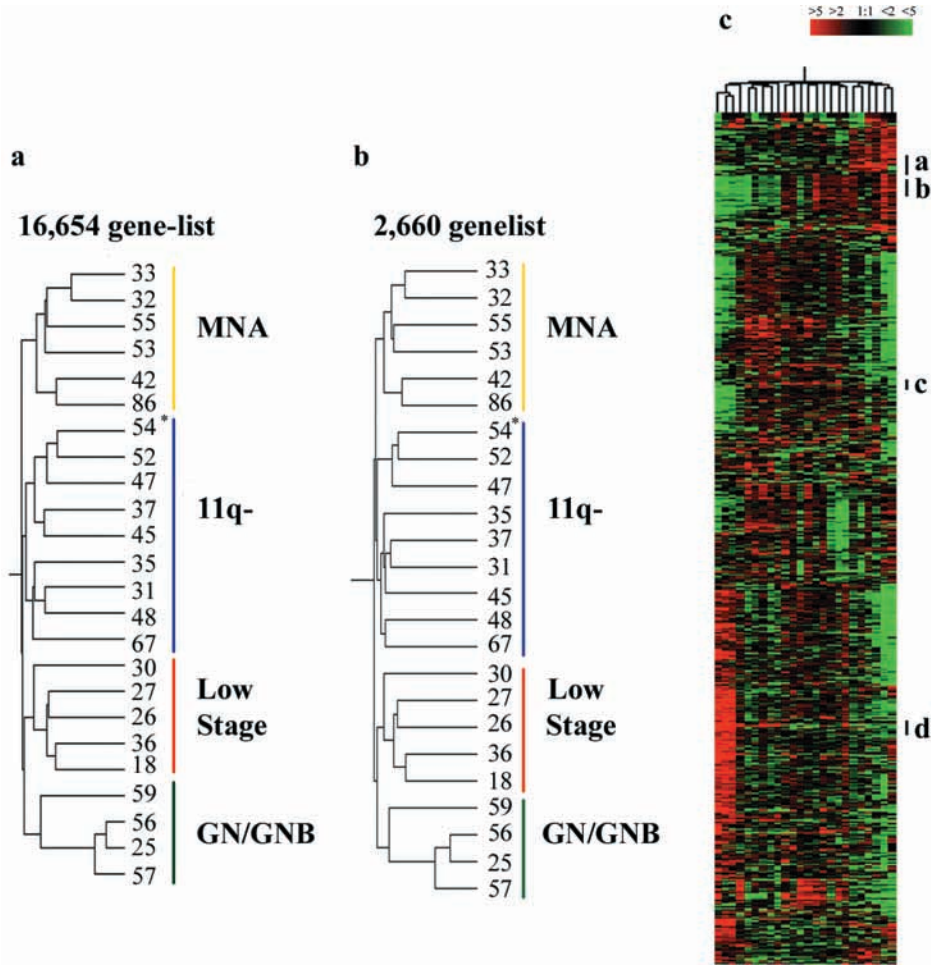

Fig. 1. Two-way hierarchical clustering analysis of gene expression data from 22 primary neuroblastic tumours and two cell lines (Kelly/N206 = sample 32; SK-N-AS = sample 33). Major groupings of tumours with similar genetic abnormalities are indicated by colour bars. (**a**) Cluster dendrogram based on the 16 654 gene-list. (**b**) Cluster dendrogram based on the 2660 transcript list. Note that some low stage 11q- tumours, including one hyperdiploid tumour (54*), cluster with the high stage 11q- tumours. (**c**) Two-way cluster analysis diagram of the 2660 transcript-list. Each row represents a single gene and each column an experimental sample. The colour represents differences in gene expression across samples. Green indicates lower than the mean expression (black), and red indicates higher than the mean expression. The sidebars to the right of the diagram represent gene clusters a to d described in the Results section. Colour scale is shown at top right.

expression relative to the standard deviation within each cluster. The statistical significance of this score is determined by permutation of the samples and significance of the score is measured in terms of a false discovery rate (FDR). The lowest FDR at which a gene is called significant is the *q* value. In this study, SAM was performed on comparing each cluster with the remaining set (one class response, unpaired data, 1000 permutations) and *q* values are given in per cent.

TaqMan quantitative reverse transcription (QRT)–PCR analysis

We used the same total RNA pools for both oligonucleotide microarray and QRT–PCR analyses. Primers and TaqMan probes for respective target genes were designed using Primer Express software (Applied Biosystems). The sequences of the various PCR primer pairs and fluorogenic probes used are indicated in Table II. Single strand cDNA was synthesized from 1 μg total RNA using the ImProm-II RT System (Promega). Each reaction was performed in duplicate by using 50 ng cDNA as template. QRT–PCR was performed using the TaqMan Universal PCR Master Mix kit (Applied Biosystems), an ABI Prism 7700 (Perkin Elmer) instrument and the following thermal cycling conditions: 2 min at 55°C and 10 min at 95°C, followed by 40 cycles of denaturation at 95°C for 15 s, annealing at 60°C for 1 min and extension at 60°C for 1 min. For comparison of transcript levels between samples, a standard curve was determined using eight serial dilutions in duplicate of a mixed cDNA template obtained from the various neuroblastoma samples under examination. Values were then normalized relative to 18s rRNA concentrations, which were obtained from a standard curve generated via use of the TaqMan 18s rRNA Control Reagents kit (Applied Biosystems).

Immunohistochemical detection of topoisomerase-II-α

A tissue microarray (TMA) was constructed using formalin-fixed paraffin-embedded samples from 20 of the tumours that were used in the oligonucleotide microarray experiments. Two 0.6 μm cores from representative areas of each tumour were used in the TMA block. Tonsil tissue was used as a positive control. Sections (4 μm thick) were cut and de-waxed in xylene, rehydrated in alcohol and blocked for endogenous activity (3% H_2O_2 and normal goat serum). Antigen retrieval was carried out by pressure-cooking in citrate buffer (pH 6.0). Sections were then incubated for 60 min at room temperature with a monoclonal anti-topoisomerase II-alpha antibody (Novocastra Laboratories Ltd, Newcastle) at a dilution of 1:30. The sections were then washed with TBS (pH 7.6) to remove unbound antisera. Bound antibody was detected using the Envision detection system (DakoCytomation) with DAB as the chromogen.

The resulting immunostained sections were examined by a single pathologist (M.McD.) in a blinded manner with a numerical counting grid using 20 and 40× objective lenses and scored using previously published methods (31). The topoisomerase labelling index (TLI) was calculated by dividing the number of positive cells by the total number of cells in the grid (average 591 cells/grid, range 60–1200). As each tumour was represented in the array as two cores, there were two TLI scores derived for each tumour.

Results

Identification of tumour subtypes by hierarchical clustering

A hierarchical clustering method was used to identify co-ordinately expressed transcripts and defined subgroups

Table II. Primers and probes used for QRT–PCR analysis

Transcript	Forward Primer (5′–3′)	Reverse primer (5′–3′)	Fluorogenic probe
MYCN	ACCATTGACACATCCGCCTT	CATGCTCCTCAAACATTGAGGTAT	FAM-CTGGGTAATGAGAGGTGGC-TTTTGCG-TAMRA
SEMA3B	GCGACACCCACTTCGATCA	CGTGGAGAAGACGGCATAGAG	FAM-CTCCAGGATGTGTTTCTGTTGT-CCTCGC-TAMRA
BIRC5	CCTTTTGCCACTGCTGTGTG	TGCCTTTTTCTGAGGGAGGA	FAM-AGACAGGCCCAGTGAGCCGCG-TAMRA
CCNA2	CCATACCTCAAGTATTTGCCATCA	GCTTTGTCCCGTGACTGTGTAG	FAM-TTGCTGGAGCTGCCTTTCATTTAGCACT-TAMRA
CDC2	AATGCTTTGAAGTATTTTTATGCTCTGA	AAAATATTCATCTTTAGCCAG-GTTGTATAG	FAM-TGTTTAAATGTTCTCATCAGTTTCTTG-CCATGTTG-TAMRA
TOP2A	TGTGATTATTTCAGCTCTTGACCTG	AAATTGGTTTCTCTCTTTGGGAGA	FAM-CCCCTCTGGCTGCCTCTGAGTCTGA-TAMRA

linked by similar patterns of gene expression (see Material and Methods). Cluster analysis of 16 654 transcripts resulted in a distinct separation of tumours with respect to stage and major genetic abnormalities (Figure 1a). As illustrated in Figure 1b, a filtered collection of 2660 differentially expressed transcripts also produced a hierarchical clustering result that was nearly identical to the result obtained using the much larger transcript set. The tumours were separated into two main branches. One branch contained the ganglioneuroma, some of the ganlioneuroblastoma (GN/GNB) tumours, and the majority of the low stage tumours (hyperdiploid and 11q-). Interestingly, two of the three 11q- tumours that were at low stage clustered with the low stage hyperdiploid tumours rather than with the high stage 11q- tumours irrespective of the fact that they had unbalanced gain of 17q. The second major branch consisted primarily of the advanced stage tumours. This branch was further subdivided into a sub-branch containing the MNA tumours and cell lines, and a sub-branch containing the high stage 11q- tumours and two low stage tumours, one that was hyperdiploid (case 54) and one that was 11q- (case 52). The MNA tumours clustered together irrespective of tumour stage; however, it is noted that this observation is based on a relatively small sample size. One of the cell lines clustering with the MNA primary tumours had MNA (Kelly/N206), while the other did not (SK-N-AS). The clustering of the SK-N-AS (not MNA) cell line with Kelly (MNA) and the MNA tumours may reflect alterations in gene expression that occurred *in vitro* and that probably promote growth in an *in vitro* environment. It should be noted that MYCN expression in Kelly was 109-fold higher than SK-N-AS, and that FISH analysis with a MYCN probe confirmed that SK-N-AS does not possess MNA (data not shown).

One tumour (case 25), originally classified as a stage 3 poorly differentiated neuroblastoma, clustered close to the ganglioneuroma. Evaluation of the post-chemotherapy sample from case 25 showed a good deal of maturation, including ganglioneuromatous areas. It would be tempting to suggest that the expression profile of the primary tumour from case 25 may have had predictive value with regards to differentiation, even though the primary tumour was classified into an unfavourable INPC prognostic category. However, maturation following chemotherapy is a common phenomenon in neuroblastoma so that the matter has clearly not been resolved by this single observation.

A subset of genes that contributed strongly to the classification of tumours depicted in Figure 1 were identified from the 2660 filtered transcript list using a number of statistical methods (see the Materials and Methods section). Hierarchical clustering with these 31 genes (Figure 2) produced a dendrogram that was very similar to that depicted in Figure 1, with only a minor variation. The 31 gene list (Figure 2) places all of the 11q- tumours in a separate cluster, irrespective of stage. The very tight clustering of the ganglioneuroma (case 57) with case 25 and case 56 is preserved, with all of the hyperdiploid low stage tumours branching from the GN/GNB cluster. The MNA tumours and cell lines form a distinct cluster that branches off from the GN/GNB/low stage hyperdiploid tumour cluster, rather than from the 11q- cluster. Table III displays additional information on the expression profiles of the 12 genes that were most strongly differentially expressed in the 11q- tumours relative to all of the other tumours used in this study. *P*-values for each gene, determined by a *t*-test, and *q* values obtained by significance analysis of microarrays, are indicated in the table.

Exploratory data mining of gene expression profiles

Hierarchical clustering revealed a number of gene expression profiles that differed between the tumour groups, providing added insight into neuroblastoma progression. A number of gene expression clusters were evident within the data. The most striking feature of the gene expression patterns identified was the great variation observed between the GN/GNB tumours compared with the neuroblastoma tumours, which is evident in Cluster D (Figure 1c). Notably within this cluster, expression of the semaphorin 3B (*SEMA3B*) gene readily distinguished between differentiated and non-differentiated tumour types. Some of the genes within this cluster may represent a potential source of markers capable of distinguishing between aggressive and indolent neuroblastic tumours. Cluster C contained a number of genes that were highly expressed in the 11q- tumours. Increased expression of these genes may be contributing to the metastatic phenotype associated with tumours displaying loss of 11q. Genes displaying similar patterns of expression to the *MYCN* gene were found in Cluster A. Cluster B (Figure 3a) contained transcripts related to cell growth and proliferation, the majority of which were up regulated in the late stage metastatic tumours. Abnormal expression of these genes may be associated with increased cellular proliferation and survival in neuroblastoma.

Validation of oligonucleotide microarray studies by TaqMan QRT–PCR and immunochemistry

In order to confirm our oligonucleotide microarray-derived findings, we carried out TaqMan QRT–PCR analysis of six

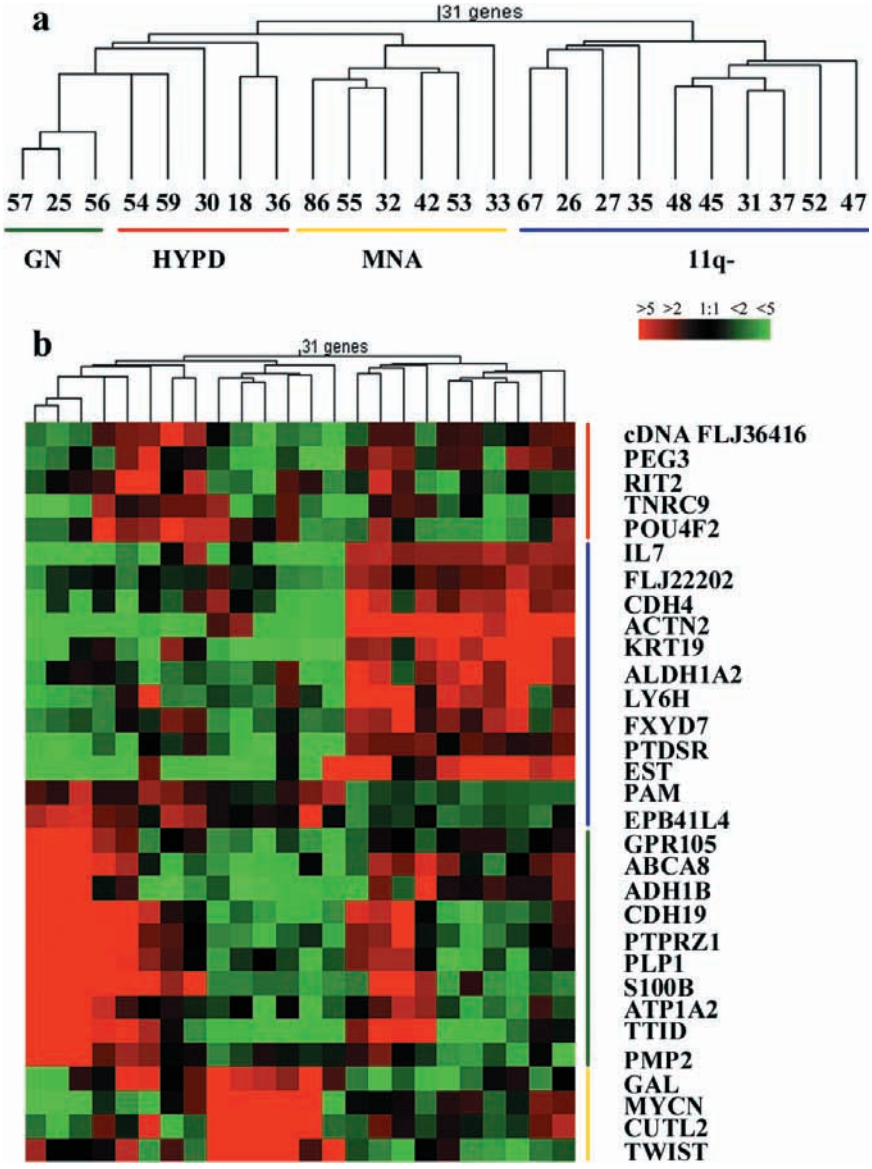

Fig. 2. Transcripts most strongly associated with the major genetic subtypes of neuroblastoma. (**a**) Cluster dendrogram based on the 31 genes that contributed most strongly to the dendrograms depicted in Figure 1. Major groupings of tumours with similar genetic abnormalities are designated with colour bars. Two cell lines (Kelly/N206 = sample 32; SK-N-AS = sample 33) are included. (**b**) Two-way cluster analysis diagram of the 31 transcript list. Genes associated with major tumour subtypes are highlighted with different colour bars (MNA tumours = yellow; GN/GNB tumours = green; 11q- tumours = blue; hyperdiploid tumours = red).

genes selected on the basis of exhibiting strong differential expression in different categories of neuroblastic tumours, such as low stage versus high stage. A subset of 14 of the 24 neuroblastoma samples was used for this purpose. The QRT–PCR results (Figure 3b–d) verified the patterns of gene expression revealed by oligonucleotide microarray analysis. In agreement with the oligonucleotide microarray data, high expression of *BIRC5*, *TOP2A*, *CCNA2* and *CDC2* was restricted to the neuroblastoma cell lines and five out of five late stage tumours, whereas, low expression of both genes was detected in one ganglioneuroma and all early stage tumours. High expression of SEMA3B was confirmed in one ganglioneuroma, while expression of this gene was almost undetectable in all neuroblastomas. In addition, expression of the *MYCN* gene was verified by QRT–PCR in this tumour subset.

To validate differential expression at the protein level, immunohistochemical staining was performed for TOP2A on a neuroblastoma TMA containing 19 of the tumour biopsies used for the oligonucleotide microarray analysis (Figure 4). Comparison of the gene expression data with the immunohistochemical staining results showed a strong correlation between *TOP2A* transcript levels and per cent of cells that were immunoreactive for this antigen (Figure 4), with the exception of one discordant result for case 53. In this respect, oligonucleotide microarray analysis of case 53 indicated a moderate level of *TOP2A* mRNA expression, whereas immunochemistry indicated that all cells examined in the core section were negative for TOP2A. A conventional section from the paraffin block of case 53, however, exhibited strongly positive areas following immunochemistry indicating that we simply sampled a negative area (partially necrotic) when constructing the TMAs.

Table III. Genes differentially expressed in 11q- neuroblastoma relative to tumours without 11q-

Gene symbol	Gene description	Chromosome location	Genebank number	GN/GNB	Hyperdiploid	11q-	MNA	*P* value[a]	*q* value[b] (%)	BGA/COA[c]
ALDH1A2	Aldehyde dehydrogenase 1 family, member A2	15q21.2	AB015228	0.9	0.6	4.6↑	0.8	0.05	0.48	+
KRT19	Keratin 19	17q21.2	NM_002276	0.4	1.1	4.2↑	0.13	0.01	0.48	+
CDH4	Cadherin 4, type 1	20q13.3	NM_001794	0.4	0.8	4.0↑	1.2	0.05	0.48	
ACTN2	Actinin, alpha 2	1q42-q43	NM_001103	0.1	0.2	5.0↑	0.9	0.001	0.56	+
n/a	Unknown protein mRNA, partial cds. similar to RIKEN cDNA B830045N13	1q31.1	BF589529	0.07	1.9	11.5↑	0.3	ns	0.48	+
IL7	Interleukin 7	8q12-q13	NM_000880	0.05	1.0	3.2↑	0.3	0.001	0.48	+
LY6H	Lymphocyte antigen 6 complex, locus H	8q24.3	NM_002347	0.3	1.7	4.5↑	0.9	ns	ns	+
FXYD7	FXYD domain containing ion transport regulator 7	19q13.11	NM_022006	0.6	1.3	3.0↑	0.6	0.05	0.48	+
PTDSR	Phosphatidylserine receptor	17q25	AA351360	0.12	0.7	2.0↑	0.5	0.01	0.48	
FLJ22202	Hypothetical protein FLJ22202	20q13.33	NM_024883	0.8	0.8	2.6↑	0.9	0.01	0.48	
PAM	Peptidylglycine alpha-amidating monooxygenase	5q14-q21	AI022882	2.8	1.6	0.7↓	1.4	0.001	0.48	
EPB41L4B	Erythrocyte membrane protein band 4.1 like 4B	9q22.1-q22.3	NM_019114	4.0	2.1	0.7↓	2.6	0.05	0.48	+

Numbers in columns under each tumour category are mean expression levels for each gene for the tumour group. There were three tumours in the GN/GNB cluster; five low stage hyperdiploid tumours; 10 tumours with 11q-; and four tumours with MNA. ns = not significant; ↑ designates increased expression in the 11q- tumours relative to the other tumour groups; ↓ designates decreased expression in the 11q- tumours relative to the other tumour groups.
[a]Computed with maxT algorithm using multtest in *R* as described in (28).
[b]Reported *q* values (%) computed with SAM. The *q* value is the lowest FDR at which a gene is called significant. In general a *q* value <5 is considered significant.
[c]Between group analysis using COA with the class groups defined. A + symbol indicates that the gene mean expression level in the 11q- tumours separated these tumours from the non-11q- tumours.
{\tf="Pi3"\char94}Although these genes were ranked among the most significant genes in both SAM and between group analysis (BGA) of data, these genes were not among genes with statistically significant adjusted *P* values using the maxT algorithm.

Validation of oligonucleotide microarray results by comparison of specific patterns of gene expression with published results

The expression patterns of genes determined by oligonucleotide microarray experimentation correlated well with expectations based on previously reported gene expression studies of neuroblastoma. For example, the mean *MYCN* expression in the MNA primary tumours was ~14-fold greater than that observed in the hyperdiploid and 11q- tumours and was absent in the (GN/GNB) tumour cluster. Two genes, *NCYM* and *DDX1*, that have been noted to sometimes co-amplify with *MYCN*, showed highly elevated expression in some of the MNA tumours (*NCYM* was highly elevated in all MNA primary tumours and in the Kelly/N206 cell line, while levels of *DDX1* was increased in case 55). Expression of the cell adhesion molecule *CD44* and the ephrin ligand *EFNB2* were significantly down regulated in the MNA tumours, consistent with previous reports (32,33). The neurotrophin receptor *NTRK1* was either absent or expressed at very low levels in the MNA tumours and expressed at significantly higher levels in the low stage hyperdiploid tumours, consistent with published expectations (34). The 11q- tumours had a mean *NTRK1* expression level that was intermediate between the low stage hyperdiploid tumours and the MNA tumours. As far as we are aware, *NTRK1* expression in GN/GNB tumours has never been reported. Curiously, *NTRK1* expression was either very low or absent in these differentiated tumours, comparable with levels of expression in the MNA tumours.

Discussion

In this study we have combined metaphase CGH and oligonucleotide microarray-based gene expression profiling technologies to further identify how physical genomic changes alter gene expression in different types of neuroblastic tumours. In particular, 12 genes were identified that are strongly differentially expressed in 11q- neuroblastoma relative to other subtypes of neuroblastic tumours. Ten of these genes have increased levels of expression in 11q- tumours, while two are down regulated (Table III). A number of the up-regulated genes have been implicated previously in oncogenesis. These included the known tumour marker KRT19 (35) and the CDH4 gene, which has recently been shown to be up-regulated in the paediatric solid tumour rhabdomyosarcoma (36). In addition, the gene encoding aldehyde dehydrogenase 1 family member A2 (ALDH1A2), an enzyme that catalyses the synthesis of retinoic acid from retinaldehyde, has been implicated in T-cell acute lymphoblastic leukaemia (37). A number of the genes showing enhanced expression in 11q- tumours, such as IL-7 and LY6H, may be indicative of an enhanced immune response and the presence of infiltrating lymphocytes in the tumour tissue. The expression patterns of the majority of the genes listed in Table III, however, never have been reported in neuroblastoma and their gene expression patterns may be contributing to the phenotype associated with loss of 11q material. None of these genes map to the chromosome 11q region, and examination of the expression patterns of all genes mapping to 11q did not identify a candidate tumour suppressor gene(s) that

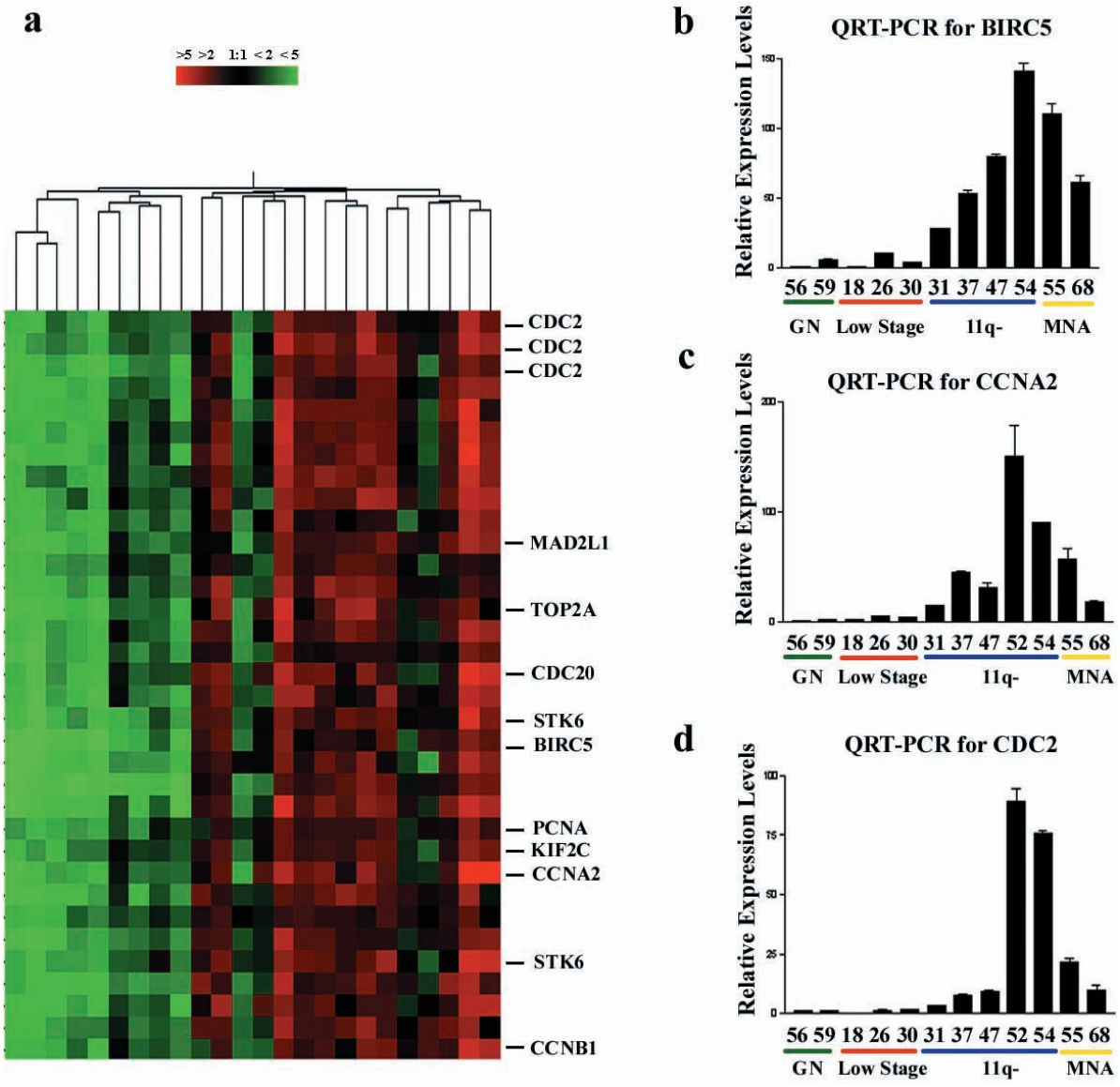

Fig. 3. Genes with increased expression in high stage versus low stage tumours. (**a**) Enlarged view of gene cluster B. The dendrogram at the top is identical to Figure 1. Cluster B contained many genes involved in proliferation and cell cycle control. Colour scale is shown at top left. (**b–d**) Confirmation by QRT–PCR of increased expression in cell lines and high stage tumours for (b) *BIRC5*, (c) *CCNA2* and (d) *CDC2*. Genes associated with major tumour subtypes are highlighted with different colour bars and exceptional tumours within these groups are discussed in the main text. Relative expression levels are shown. Data shown are averages of duplicate experiments and associated standard errors are plotted.

is targeted by loss of heterozygosity on this chromosome. The 11q tumour suppressor gene, however, might not have a large enough change in expression to be detectable by microarray analysis, particularly if the tumorigenic effect is a consequence of haploinsufficiency. Loss of expression of this tumour suppressor gene nevertheless could have a profound effect on the expression of other genes, which is perhaps evidenced by the fact that a number of genes located throughout the genome have expression profiles that are associated with loss of 11q. Additional experiments, designed to determine if loss of 11q material is causally related to the gene expression patterns that are unique to 11q- tumours would be of considerable interest.

Hierarchical cluster analysis permitted us to distinguish four major genetic subtypes of neuroblastic tumours, namely GN/GNB tumours, low stage tumours possessing either hyperdiploidy or loss of 11q, high stage tumours with 11q loss and tumours with MNA (irrespective of stage). Clustering did not permit us to differentiate between 11q- tumours with and without loss of 3p, and it was not possible to correlate any pattern of gene expression with loss of 3p. This indicates that loss of 11q may contribute to alterations in global gene expression in a more significant manner than does loss of chromosome 3p; bearing in mind that the number of 3p- tumours included in the present study was small. Although loss of 3p may not have a major impact on the expression of genes on many different chromosomes, it could still play a significant role in neuroblastoma progression or differentiation.

Hierarchical cluster analysis classified tumours based on overall similarity in their gene expression patterns, reflecting the relationships that exist between the tumours. Two lower stage tumours (stage 1 and stage 2) with loss of 11q and unbalanced gain of 17q (cases 26 and 27) clustered with the hyperdiploid low stage tumours as opposed to the higher stage 11q- tumours when the expanded set of

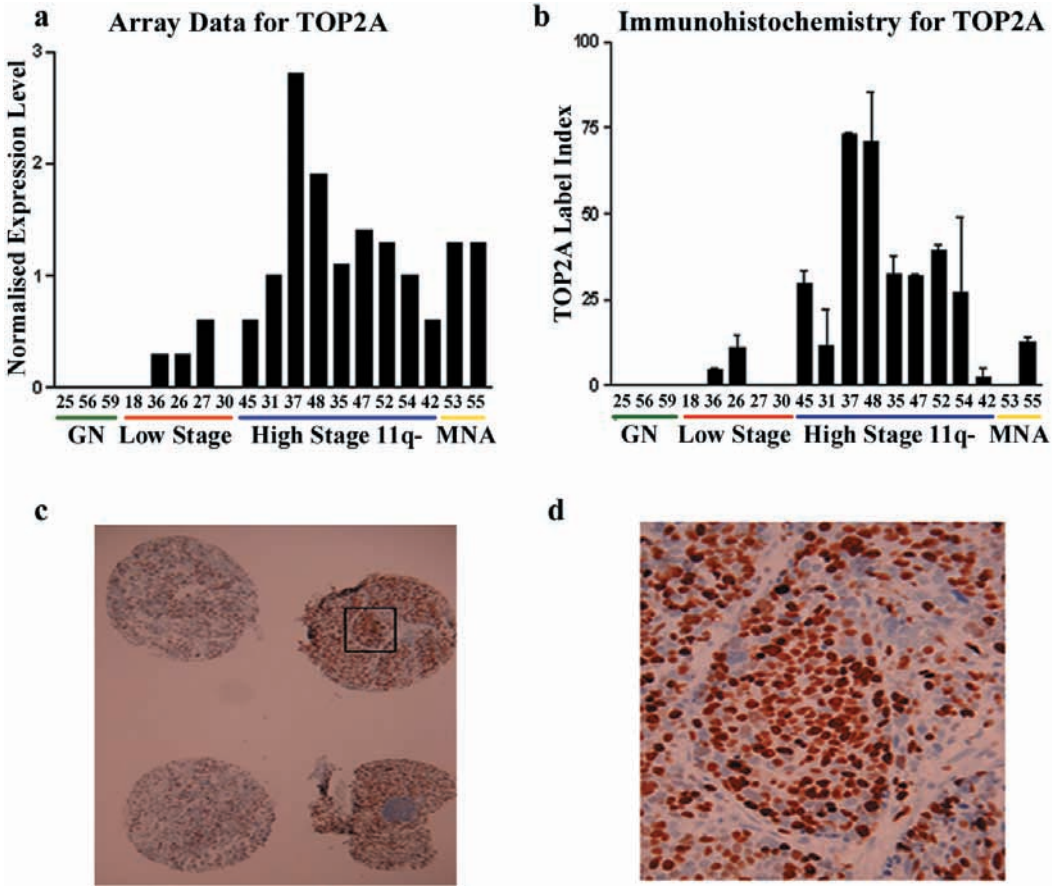

Fig. 4. Confirmation of increased expression of *TOP2A* in high stage neuroblastoma tumours. (**a**) oligonucleotide microarray expression data for *TOP2A* in 19 neuroblastic tumours. Normalized expression levels are shown. Genes associated with major tumour subtypes are highlighted with different colour bars and exceptional tumours within these groups are discussed in the main text (**b**) Immunohistochemical detection of TOP2A in 19 neuroblastic tumours in the neuroblastoma tissue microarray. The TOP2A labelling index is shown. Each tumour was represented twice in the array. Data shown are averages and associated standard errors are plotted. (**c**) Representative examples of immunohistochemical staining of neuroblastoma TMA using an antibody against TOP2A. Upper and lower left: moderate staining for TOP2A (replicates for case 45). Upper and lower right: strong staining for TOP2A (replicates for case 37). (**d**) Enlarged view of tumour section from region designated in (**c**), illustrating positive and negative cells for TOP2A staining, case 37.

differentially expressed transcripts was used. Both of these patients are alive and have had no relapse events for 3 and 4 years, in spite of the fact that they have genomic abnormalities indicative of a poor clinical outcome. It is intriguing to speculate that loss of 11q, and gain of 17q material are insufficient events to lead to a global gene expression profile indicative of stage 4 neuroblastoma. This leads us to suggest that additional events, perhaps epigenetic in nature, are required for tumour progression and metastasis.

Ramaswamy *et al*. (38) recently published a seminal microarray study of gene expression in unmatched primary and metastatic adenocarcinomas from diverse tissue sources. These investigators identified a gene expression signature (based on 17 genes) that distinguished primary tumour from metastatic tumour. A subset of the primary tumours displayed gene expression profiles that were more similar to the profiles of the metastatic tumours than the other primary tumours, leading the authors to conclude that the metastatic potential is encoded within the bulk of the primary tumour. This challenges the notion that metastatic cells arise from rare cells within primary tumour (39). Ramaswamy *et al*. (38) also applied their 17-gene expression signature to the analysis of medulloblastoma and found that this cohort of genes provided a high level of discrimination between primary and metastatic tumours. We performed hierarchical cluster analysis with these 17 genes on our panel of neuroblastoma tumours, but found that this set of genes provided no discrimination between low stage and high stage tumours, or between the different genetic subtypes using GeneSpring software and our parameters for data normalization (data not shown). This result leads us to conclude that the metastatic expression signature provided by this set of genes may not be universally applicable to all types of tumours.

Two lower stage tumours, case 52 (11q-/stage 2) and case 54 (hyperdiploid/stage) clustered with the higher stage 11q- tumours in our data set. Interestingly, these two tumours also displayed an increased expression of the cell cycle genes *CCNA2* and *CDC2* as well as *BIRC5* (survivin) and *TOP2A*, which appear to be associated with a more advanced stage of disease. It seems that these low stage tumours have expression profiles that correlate stronger with the advanced stage tumours and may provide further support to the concept that metastatic potential can be encoded within the bulk of the primary tumour at an early stage.

Our oligonucleotide microarray studies also provide additional novel insight into the expression of many different

genes in different neuroblastoma subtypes. For example, Perel *et al*. (40) have demonstrated by *in situ* hybridization and immunofluorescence studies that galanin (GAL), which encodes for a short peptide of 29 or 30 amino acids, is expressed at much higher levels in neuroblastoma than in ganglioneuroma. Our results indicate that *GAL* is expressed at significantly higher levels in only some of the genetic subtypes of neuroblastoma relative to ganglioneuroma. Most notably, MNA tumours and low stage hyperdiploid tumours exhibited significantly higher *GAL* expression than what was detected in the ganglioneuroma cluster. Interestingly, *GAL* clustered very closely to the *MYCN* gene. *GAL* expression in the 11q- neuroblastoma, however, was reduced to levels that are comparable with ganglioneuroma. Peral *et al*. (40) did not report on the status of 11q in their non-MNA amplified tumours, which is probably why this observation was not noted. Our result indicates that strong down regulation of *GAL* expression is not confined to ganglioneuroma and for this reason may not be an accurate indicator of tumour differentiation.

A number of genes were highly expressed in the GN/GNB tumours versus the malignant tumours in which a signal was almost undetectable. Some of these genes, such as semaphorin 3b (*SEMA3B*) may be crucial tumour suppressor genes in neuroblastoma and loss of expression may be contributing to tumorigenesis and metastatic potential. *SEMA3B* plays a role in axonal guidance in neurons of the sympathetic nervous system and has recently been shown to play a role in the suppression of tumorigenicity in certain lung and ovarian cancer cell lines (41,42). *SEMA3B* was highly expressed in GN/GNB tumours, and was either not expressed or only very weakly expressed in all of the malignant tumours irrespective of stage or genetic abnormality. Although *SEMA3B* maps to the 3p21 region that is frequently deleted in neuroblastoma (particularly in the 11q- subtype), its expression could not be correlated with 3p deletion, due to the very weak expression. Nevertheless, the association of *SEMA3B* expression with differentiation of neuroblastic tumours, and its absence in poorly differentiated neuroblastoma suggests that this gene could potentially be a good marker for assessing whether neuroblastoma may differentiate. A number of other potentially interesting genes were contained within this cluster including *S100B* and *NDRG2*. S100 proteins are localized in the cytoplasm and/or nucleus of a wide range of cells, and are involved in the regulation of a number of cellular processes such as cell cycle progression and differentiation. A previous study, which measured S100B by immunoassay, reported lower levels of the protein in patients with undifferentiated neuroblastomas (43). NDRG2 is a member of the MYCN down regulated gene family and has recently been implicated in cell differentiation (44). Absence of these genes in poorly differentiated neuroblastoma suggests that they could potentially be good markers for assessing whether neuroblastoma may differentiate. Taken together these results suggest a possible role for *SEMA3B*, *S100B* and *NDRG2* in the differentiation of neuroblastic tumours. However, analysis of additional tumours will be required to verify these results.

Examination of the differentially expressed gene clusters identified a number of genes that appeared to have a stage related pattern of expression. These included a number of cell cycle related genes including *CCNA2* and *CDC2*, among others. The products of both of these genes were increased significantly in high stage tumours. Other genes displaying increased levels of expression in the high stage versus low stage tumours as determined by oligonucleotide microarray analysis included *BIRC5* and *TOP2A*. These genes map to 17q25 and 17q21-22, respectively, which falls into a region consistently gained in high stage neuroblastoma. Increased expression of *BIRC5* in advanced stage neuroblastoma has been reported previously (45). Our results imply that increased *TOP2A* expression may also be part of the phenotype for malignant neuroblastoma cells. The gene encoding this enzyme functions as the target for several anticancer agents. A recent study reported that etoposide, a TOP2A inhibitor, induced apoptotic alterations in a neuroblastoma cell line (46). Our results suggest that therapeutic options for neuroblastoma could therefore include appropriate topoisomerase II alpha-targeted drugs.

The classification of human cancers into prognostically significant groups is extremely important for optimal patient management. Although we have only discussed a fraction of the genes that varied in expression between the different genetic subtypes of neuroblastoma, the gene expression signatures discovered by our oligonucleotide microarray approach identified a number of potentially important genes. The proteins encoding these genes may represent new targets for improving neuroblastoma diagnosis and treatment. A more detailed analysis of individual genes may allow a more complete understanding of this disease. Many of the genes mentioned here clearly deserve high priority in future studies of neuroblastoma.

Acknowledgements

This work was supported in part by a grant from the Children's Medical and Research Foundation in Ireland (RLS).

References

1. Brodeur,G.M. (2003) Neuroblastoma: biological insights into a clinical enigma. *Nat. Rev. Cancer*, **3**, 203–16.
2. Brinkschmidt,C., Christtiansen,H., Terpe,H.J., Simon,R., Boecker,W., Lampert,F. and Stoerkel,S. (1997) Comparative genomic hybridization (CGH) analysis of neuroblastomas—an important methodological approach in paediatric tumor pathology. *J. Pathol*., **181**, 394–400.
3. Lastowska,M., Nacheva,E., McGuckin,A., Curtis,A., Grace,C., Pearson,A. and Bown,N. (1997) Comparative genomic hybridization study of primary neuroblastoma tumors. *Genes Chromosomes Cancer*, **18**, 162–169.
4. Vandesompele,J., Van Roy,N., Van Gele,M. *et al*. (1998) Genetic heterogeneity of neuroblastoma studied by comparative genomic hybridization. *Genes Chromosomes Cancer*, **23**, 141–152.
5. Plantaz,D., Vandesompele,J., Van Roy,N. *et al*. (2001) Comparative genomic hybridization (CGH) analysis of stage 4 neuroblastoma reveals high frequency of 11q deletion in tumors lacking *MYCN* amplification. *Int. J. Cancer*, **91**, 680–686.
6. Breen,C.J., O'Meara A., McDermott.,M., Mullarkey,M. and Stallings,R.L. (2000) Co-ordinate deletion of chromosome 3p and 11q in neuroblastoma detected by comparative genomic hybridization. *Cancer Genetic Cytogenet*., **120**, 44–49.
7. Guo,C., White,P.S., Weiss,M.J. *et al*. (1999) Allelic deletion at 11q23 is common in *MYCN* single copy neuroblastomas. *Oncogene*, **18**, 4948–4957.
8. Spitz,R., Hero,B., Ernestus,K. and Berthold,F. (2003) Deletions in chromosome arms 3p and 11q are new prognostic markers in localized and 4s neuroblastoma. *Clin. Can. Res*., **9**, 52–58.
9. Alaminos,M., Mora,J., Cheung,N.K.V., Smith,A., Qin,J., Chen,L. and Gerald,W.L. (2003) Genome-wide analysis of gene expression associated with MYCN in human neuroblastoma. *Cancer Res*., **63**, 4538–4546.

10. Boon,K., Caron,H.N., van Asperen,R. *et al*. (2001) N-MYC enhances the expression of a large set of genes functioning in ribosome biogenesis and protein synthesis. *EMBO J*., **20**, 1383–1393.
11. Spieker,N., van Sluis,P., Beitsma,M., Boon,K., van Schaik,B.D., van Kamp,A.H., Caron,H. and Versteeg,R. (2001) The meis1 oncogene is highly expressed in neuroblastoma and amplified in cell line imr32. *Genomics*, **71**, 214–221.
12. Khan,J., Wei,J.S., Ringner,M. *et al*. (2001) Classification and diagnostic prediction of cancers using gene expression profiling and artificial neural networks. *Nature Med*., **7**, 673–679.
13. Yamanaka,Y., Hamazaki,Y., Sato,Y., Ito,K., Watanabe,K., Heike,T., Nakahata,T. and Nakamura,Y. (2002) Maturational sequence of neuroblastoma revealed by molecular analysis on cDNA microarrays. *Int. J. Oncol*., **21**, 803–807.
14. Mora,J., Gerald,W.L. and Cheung, N-K.V. (2003) Evolving significance of prognostic markers associated with new treatment stratagies in neuroblastoma. *Cancer Lett*., **197**, 119–124.
15. Hiyama,E., Hiyama,K., Yamaoka,H., Sued,T., Reynolds,C.P. and Yokoyama,T. (2004) Expression profiling of favorable and unfavourable neuroblastoma. *Pediatr. Surg. Int*., **20**, 33–38
16. Phillips,J.L., Hayward,S.W., Wang,Y. *et al*. (2001) The consequences of chromosomal aneuploidy on gene expression profiles in a cell line model for prostate carcinogenesis. *Cancer Res*., **61**, 8143–8149.
17. Pollack,J.R., Sorlie,T., Perou,C.M., Rees,C.A., Jeffrey,S.S., Lonning,P.E., Tibshirani,R., Botstein,D., Borresen-Dale,A.L. and Brown,P.O. (2002) Microarray analysis reveals a major direct role of DNA copy number alteration in the transcriptional program of human breast tumors. *Proc. Natl Acad. Sci. USA*, **99**, 12963–12968.
18. Li,R., Sonik,A., Stindl,R., Rasnick,D. and Duesberg,P. (2000) Aneuploidy vs gene mutation hypothesis of cancer: recent study claims mutation but is found to support aneuploidy. *Proc. Natl Acad. Sci. USA*, **97**, 3236–3241.
19. Shimada,H., Ambros,I.M., Dehner,L.P. *et al*. (1999) The international neuroblastoma pathology classification (the Shimada system). *Cancer*, **86**, 364–72.
20. Shimada,H., Ambros,I.M., Dehner,L.P., Hata,J., Joshi,V.V. and Roald,B. (1999) Terminology and morphologic criteria of neuroblastic tumors: recommendations by the international neuroblastoma pathology committee. *Cancer*, **86**, 349–63.
21. Stallings,R.L., Howard,J., Dunlop,A., Mullarkey,M., McDermott,M., Breatnach,F. and O'Meara,A. (2003) Are gains of chromosomal regions 7q and 11p important abnormalities in neuroblastoma? *Cancer Genetic Cytogenet*., **140**, 133–137.
22. Breen,C.J., Barton,L., Carey,A. *et al*. (1999) Applications of comparative genomic hybridization in constitutional chromosome studies. *J. Med. Genet*., **36**, 511–517.
23. Irizarry,R.A., Hobbs,B., Collin,F., Beazer-Barclay,Y.D., Antonellis,K.J., Scherf,U. and Speed,T.P. (2003) Exploration, normalization and summaries of high density DNA array probe level data. *Biostatistics*, **4**, 249–264.
24. Schadt,E.E., Li,C., Ellis,B. and Wong,W.H. (2001) Feature extraction and normalization algorithms for high-density DNA gene expression array data. *J. Cell Biochem. Suppl*., **37**, 120–125.
25. Fellenberg,K., Hauser,N.C., Brors,B., Neutzne,A., Hoheisel,J.D. and Vingron,M. (2001) Correspondence analysis applied to microarray data. *Proc. Natl Acad. Sci. USA*, **98**, 10781–10786.
26. Culhane,A.C., Perriere,G., Considine,E.C., Cotter,T.G. and Higgins,D.G. (2002) Between-group analysis of microarray data. *Bioinformatics*, **18**, 1600–1608.
27. Thiolouse,J., Chessel,D., Doledec,S. and Olivier,J.M. (1997) ADE-4 a multivariateanalysis and graphical display software. *Stat. Comput*., **7**, 75–83.
28. Ge,Y., Dudoit,S. and Speed,T.P. (2003) Resampling-based multiple testingfor microarray data analysis. TEST, Vol. 12, No. 1, p. 1–44 (plus discussion pp. 44–77) (http://www.stat.Berkeley.EDU/tech-reports/index.html Tech report #633).
29. Tusher,V.G, Tibshirani,R. and Chu,G. (2001) Significance analysis of microarrays applied to the ionizing radiation response**.** *Proc. Natl Acad. Sci. USA*, **98**, 5116–5121.
30. Storey,J.D. and Tibshirani,R. (2003) Statistical significance for genome-wide studies. *Proc. Natl Acad. Sci. USA*, **100**, 9440–9445.
31. Park,S.-H. and Suh,Y.-L. (2003) Expression of cyclin A and topoisomerase IIa, of oligodendrogliomas is correlated with tumour grade, MIB-1 labelling index and survival. *Histopathology*, **42**, 395–402.
32. Gross,N., Beretta,C., Peruisseau,G., Jackson,D., Simmons,D. and Beck,D. (1994) CD44H expression by human neuroblastoma cells: relation to MYCN amplification and lineage differentiation. *Cancer Res*., **54**, 4238–4242.
33. Tang,X.X., Evans,A.E., Zhao,H., Cnaan,A., London,W., Cohn,S.L., Brodeur,G.M. and Ikegaki,N. (1999) High-level expression of EpHB6, EFNB2 and EFNB3 is associated with low tumor stage and high TrkA expression in human neuroblastoma. *Clin. Cancer Res*., **5**, 1491–1496.
34. Nakagawara,A., Arima,M., Aza,C.G., Scavarda,N.J. and Brodeur,G.M. (1992) Inverse relationship between trk expression and N-myc amplification in human neuroblastomas *Cancer Res*., **52**, 1364–1368.
35. Wikman,H., Kettunen,E., Seppanen,J.K., Karjalainen,A., Hollmen,J., Anttila,S. and Knuutila,S. (2002) Identification of differentially expressed genes in pulmonary adenocarcinoma by using cDNA array. *Oncogene*, **21**, 5804–5813.
36. Charrasse,S., Comunale,F., Gilber,E., Delattre,O. and Gauthier-Rouviere,C. (2003) Variation in cadherins and catenins expression is linked to both proliferation and transformation of Rhabdomyosarcoma. *Oncogene*, **23**, 2420–2430.
37. Ono,Y., Fukuhara,N. and Yoshie,O. (1998) TAL1 and LIM-only proteins synergistically induce retinaldehyde dehydrogenase 2 expression in T-cell acute lymphoblastic leukemia by acting as cofactors for GATA3. *Mol. Cell. Biol*., **18**, 6939–6950.
38. Ramaswamy,S., Ross,K.N., Lander,E.S. and Golub,T.R. (2003) A molecular signature of metastasis in primary solid tumors. *Nature Genet*., **33**, 49–54.
39. Fidler,I.J. and Kripke,M.L. (1977) Metastasis results from pre-existing variant cells within a malignant tumor. *Science*, **197**, 893–895.
40. Perel,Y., Amrein,L., Dobremez,E., Rivel,J., Daniel,J.Y. and Landry,M. (2002) Galanin receptor expression in neuroblastic tumours: correlation with their differentiation status. *Br. J. Cancer*, **86**, 117–122.
41. Tomizawa,Y., Sekido,Y., Kondo,M., Gao,B., Yokota,J., Roche,J., Drabkin,H., Lerman M.I., Gazdar,A.F. and Minna,J.D. (2001) Inhibition of lung cancer cell growth and induction of apoptosis after reexpression of 3p21.3 candidate tumor suppressor gene SEMA3B. *Proc. Natl Acad. Sci. USA*, **98**, 13954–13959.
42. Tse,C., Xiang,R., Bracht,T. and Naylor,S.L. (2002) Human semaphorin 3B located at chromosome 3p21.3 suppresses tumor formation in an adenocarcinoma cell line. *Cancer Res*., **62**, 542–546.
43. Ishiguro,Y., Kato,K., Akatsuka,H., Iwata,H., Ito,F., Watanabe,Y. and Nagaya,M. (1996) Comparison of calbindin D-28k and S-100 protein B in neuroblastoma as determined by enzyme immunoassay. *Jpn. J. Cancer Res*., **87**, 62–7.
44. Qu,X., Zhai,Y., Wei,H., Zhang,C., Xing,G., Yu,Y. and He,F. (2002) Characterization and expression of three novel differentiation-related genes belong to the human NDRG gene family. *Mol. Cell. Biochem*., **229**, 35–44.
45. Islam,A., Kageyama,H., Takada,N. *et al*. (2000)High expression of Survivin, mapped to 17q25, is significantly associated with poor prognostic factors and promotes cell survival in human neuroblastoma. *Oncogene*, **19**, 617–623.
46. Bursztajn,S., Feng,J.J., Nanda,A. and Berman,S.A. (2001) Differential responses of human neuroblastoma and glioblastoma to apoptosis. *Brain Res. Mol. Brain Res*., **91**, 57–72.

Received February 27, 2004; revised April 8, 2004; accepted April 9, 2004